



## Studying the vertical variation of cloud droplet effective radius using ship and space-borne remote sensing data

Ruiyue Chen,<sup>1,2</sup> Robert Wood,<sup>3</sup> Zhanqing Li,<sup>1,2</sup> Ralph Ferraro,<sup>2,4</sup> and Fu-Lung Chang,<sup>5</sup>

Received 12 November 2007; revised 28 February 2008; accepted 2 May 2008; published 25 July 2008.

[1] The albedo of marine stratocumuli depends upon cloud liquid water content, droplet effective radius ( $r_e$ ), and how these parameters vary with height. Using satellite data and shipborne data from the East Pacific Investigation of Climate (EPIC) Stratocumulus Study, this study investigates the cloud  $r_e$  vertical variation for drizzling and nondrizzling clouds. Visible/near-infrared retrievals from the NASA Moderate Resolution Imaging Spectroradiometer (MODIS) are used to estimate the vertical profile of  $r_e$ . MODIS  $r_e$  observations and collocated shipborne scanning C-band precipitation radar data show that  $r_e$  generally increases with height in nondrizzling clouds, consistent with aircraft observations. It is found that in clouds with precipitation rates greater than a few hundredths of a  $\text{mm h}^{-1}$  the vertical gradient of  $r_e$  is significantly less than that in nondrizzling clouds and can become negative when the drizzle is heavier than approximately  $0.1 \text{ mm h}^{-1}$ . High values of  $r_e$  at drizzling cloud base are consistent with estimates of the ratio of liquid water in the drizzle drops to that in the cloud droplets. C-band derived cloud base precipitation rates are found to be better correlated with  $r_e$  at cloud base than with  $r_e$  at cloud top, suggesting that passive remote sensing may be useful for drizzle detection.

**Citation:** Chen, R., R. Wood, Z. Li, R. Ferraro, and F.-L. Chang (2008), Studying the vertical variation of cloud droplet effective radius using ship and space-borne remote sensing data, *J. Geophys. Res.*, 113, D00A02, doi:10.1029/2007JD009596.

### 1. Introduction

[2] Low-level stratiform liquid water clouds have a significant influence on the Earth's climate due to their strong shortwave radiative forcing [Greenwald *et al.*, 1995]. Such clouds cover large regions of the Earth's oceans [Klein and Hartmann, 1993]. The shortwave optical depth of liquid water clouds depends upon both the bulk condensate amount and the size of the cloud drops. Dependence on the latter is conveniently expressed as an effective radius which is the ratio of the third to second moments of the cloud droplet size distribution.

[3] The vertical variation of cloud droplet effective radius ( $r_e$ ) is an important cloud property which reflects both condensation and coalescence growth. There are different ways to obtain information on the vertical profile of cloud  $r_e$ , including in situ aircraft measurements [e.g., Martin *et al.*, 1994; Wood, 2000; Miles *et al.*, 2000] and new retrievals from satellite measurements of solar reflectance [Chang and

Li, 2002]. The aircraft measurements in low clouds show that  $r_e$  generally increases with height for nondrizzling clouds [Martin *et al.*, 1994; Miles *et al.*, 2000; Wood, 2000] but that drizzle drops start to increase the effective radius significantly if the liquid water content of drizzle drops is above 5–10% of the liquid water content of small cloud droplets [Wood, 2000]. These drizzle droplets thus reduce the vertical gradient and even lead to  $r_e$  decreasing with height because drizzle drops tend to increase in size toward the base of the cloud [Wood, 2005a]. However, only limited work has been carried out to examine the vertical profile of effective radius in drizzling low clouds. Drizzle commonly occurs in marine low clouds and its effects upon cloud optical properties are very poorly understood [Albrecht, 1989; Wood, 2005a; Comstock *et al.*, 2004; VanZanten *et al.*, 2005].

[4] Satellite observation is the only practical way to infer cloud  $r_e$  globally. Solar reflectance measurements from a visible channel and a near infrared (NIR) channel are widely used to estimate cloud optical depth and cloud top  $r_e$  [Nakajima and King, 1990; Han *et al.*, 1994]. Using radar and a solar/infrared radiometer on board the Tropical Rainfall Measuring Mission (TRMM), Kobayashi [2007] found that cloud  $r_e$  of precipitating clouds is obviously larger than that for nonprecipitating clouds. In previous studies, cloud  $r_e$  retrievals have used three NIR channels, which have wavelengths of  $\lambda = 1.6 \mu\text{m}$ ,  $2.1 \mu\text{m}$ , and  $3.7 \mu\text{m}$  [King *et al.*, 2003]. Because clouds absorption is different at the three wavelengths, the NIR channels have different reflectance weighting functions from cloud top to cloud

<sup>1</sup>Department of Atmospheric and Oceanic Sciences, University of Maryland, College Park, Maryland, USA.

<sup>2</sup>Cooperative Institute for Climate Studies, University of Maryland, College Park, Maryland, USA.

<sup>3</sup>Department of Atmospheric Sciences, University of Washington, Seattle, Washington, USA.

<sup>4</sup>Center for Satellite Applications and Research, NESDIS, NOAA, Camp Springs, Maryland, USA.

<sup>5</sup>National Institute for Aerospace, Hampton, Virginia, USA.

base. *Platnick* [2000] found the weighting function for  $\lambda = 3.7 \mu\text{m}$  is mainly confined to the cloud top layer (i.e., within optical depth 2) and sharply decrease toward cloud base, while the weighting function at  $\lambda = 1.6 \mu\text{m}$  spreads more evenly into the lower cloud layer (i.e., for a cloud with optical depth equal to 8, the weighting function value at cloud base is around half of its maximum value). Consequently, the  $\lambda = 3.7 \mu\text{m}$  retrieval corresponds to the  $r_e$  close to the top of the cloud layer, whereas the  $\lambda = 2.1 \mu\text{m}$  and  $\lambda = 1.6 \mu\text{m}$  retrievals are sensitive to  $r_e$  values deeper inside the cloud. Assuming that the  $r_e$  has a linear distribution in the vertical direction, *Chang and Li* [2002, 2003, hereinafter referred to as CL] present a method to determine an optimal linear  $r_e$  profile by using a combination of NIR measurements at  $\lambda = 3.7 \mu\text{m}$ ,  $2.1 \mu\text{m}$ , and  $1.6 \mu\text{m}$ . The linear  $r_e$  assumption is based on many  $r_e$  profile measurements worldwide [*Miles et al.*, 2000; *Wood*, 2000; *Brenguier et al.*, 2000].

[5] Applying the CL algorithm to reflectance measurements from the Moderate Resolution Imaging Spectroradiometer (MODIS) on the NASA Aqua satellite, *Chen et al.* [2007] conducted a preliminary study to show that the distributions of  $r_e$  profile are different for drizzling and nondrizzling clouds. However, the definition of drizzling used in their study was based on an empirical threshold of liquid water path (LWP), which is retrieved from brightness temperature measurements from the Advanced Microwave Scanning Radiometer (AMSR-E) on Aqua. The threshold-based detection of drizzling suffers from an ambiguity caused by cloud LWP (i.e., it is not clear how to separate the detected LWP into cloud and rain components) and has difficulty detecting light drizzle [*Zuidema et al.*, 2005]. Failure to detect light drizzle could also be caused by the nearly  $100 \text{ km}^2$  field of view size of AMSR-E 37 GHz channel, which is the primary channel used in LWP estimation [*Ashcroft and Wentz*, 2000].

[6] In this study, measurements from the East Pacific Investigation of Climate (EPIC) Stratocumulus Study are used for cloud profile analysis. Coincident radiance measurements from MODIS on the Terra satellite are used to estimate the  $r_e$  profile with the CL algorithm. Through a synergistic analysis of radar reflectivity profile measured by a millimeter cloud radar (MMCR), drizzle measurements from a scanning C-band radar, and satellite estimation of the (assumed linear)  $r_e$  profile, the vertical variation of cloud  $r_e$  is estimated for both drizzling and nondrizzling clouds. Such analysis was not possible in previous studies because of the lack of observation of cloud  $r_e$  profile and drizzle. The estimation of vertical  $r_e$  variation and how it depends upon the drizzle rate provide useful information for drizzle detection, cloud modeling, and climate studies (i.e., study of aerosol indirect effect).

[7] Section 2 introduces the instruments that are used in this study and the data processing methods. The uncertainties of the data from these instruments are also discussed. In section 3, estimates of the partitioning of liquid water content between drizzle drops and small cloud droplets is carried out using MMCR data in drizzling stratocumulus by incorporating simultaneous LWP estimates from a passive microwave radiometer. Drizzle precipitation rates obtained from the C-band radar and spatiotemporally matched  $r_e$  profile estimation from MODIS satellite measurements are

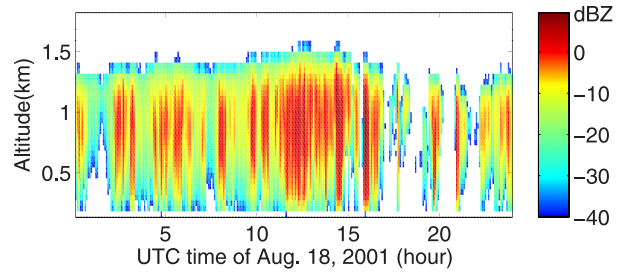


**Figure 1.** Millimeter cloud radar reflectivity measurements on 18 October 2001.

combined to evaluate the impact of drizzle on the trend of vertical  $r_e$  variation. Section 4 summarizes the result of this study, discusses the potential of profile retrieval on drizzle detection, and presents further research need to be done in the future.

## 2. Data and Methods

[8] The EPIC Stratocumulus Study [*Bretherton et al.*, 2004] was conducted in October 2001 within the southeastern Pacific stratocumulus region. From 16 to 22 October, the NOAA research vessel R/V *Ronald Brown* (RHB) was stationary at  $20^\circ\text{S}$ ,  $85^\circ\text{W}$  and observed a relatively well-mixed boundary layer with predominantly overcast skies and few upper level clouds. Comprehensive cloud and precipitation measurements were taken by vertically pointing remote sensing instruments on the RHB. This investigation uses cloud profile and drizzle estimates at  $20^\circ\text{S}$ ,  $85^\circ\text{W}$  from EPIC instruments, as well as  $r_e$  profile estimation from spatiotemporally matched data from MODIS on Terra.

### 2.1. Cloud Measurements From Millimeter Radar, Ceilometer, and Microwave Radiometer

[9] Cloud reflectivity profiles are provided by vertically pointing 8.6mm wavelength radar (MMCR), which has a vertical resolution of 45 m [*Moran et al.*, 1998]. The beam width is  $0.5^\circ$  and the minimum detectable reflectivity is around  $-60 \text{ dBZ}$ . The radar obtains a reflectivity profile every 10 s, but the reflectivity profile measurements are averaged to a 5 min temporal resolution for this study (equivalent to approximately 5 km horizontal spatial resolution). The calibration error of MMCR data are less than 1 dBZ. *Comstock et al.* [2004] showed that the uncertainty of the MMCR radar measurements caused by Mie scattering is less than 10% for stratocumulus clouds given the mean radii of cloud and drizzle drops encountered in EPIC. Cloud top height is determined using a reflectivity threshold of  $-40 \text{ dBZ}$  to define cloud, a value that leads to cloud top heights very close to the height of the inversion base as determined using radiosondes (not shown). The cloud base height is measured using a ceilometer with 15 m vertical resolution. The LWP is estimated from brightness temperature measurements of a microwave radiometer at 22 GHz and 31 GHz [*Zuidema et al.*, 2005]. The uncertainty of the LWP estimation is around  $10\text{--}25 \text{ g}^{-2}$ . Figure 1 shows an example of MMCR reflectivity measurements for a 24 h period (18 October 2001) in which significant drizzle was observed to fall [see *Comstock et al.*, 2004]. In this study,

estimates of the partitioning of liquid water content between drizzle drops and small cloud droplets is carried out using MMCR data in stratocumulus by incorporating simultaneous LWP estimates from a passive microwave radiometer.

## 2.2. Estimates of Drizzle From Scanning C-Band Radar

[10] The C-band radar on the RHB has a 5 cm wavelength and 0.95° beam width. During EPIC, the C-band completed an 11-elevation angle volumetric scan out to 30 km radius every 5 min [Comstock *et al.*, 2004]. Reflectivity between 0.5 km and 2 km altitude is averaged to produce two-dimensional maps with an estimated calibration error of  $\pm 2.5$  dBZ. The minimum detectable reflectivity is approximately  $-12$  dBZ at 30 km distance. Because of its sensitivity, C-band measurements in low water clouds are only sensitive to drizzle, as cloud liquid water content cannot produce the reflectivity at sufficient magnitude to be detected. In this study, the cloud base precipitation rate is estimated using  $Z = 25R^{1.3}$ , where  $Z$  is the radar reflectivity in  $\text{mm}^6\text{m}^{-3}$ , and  $R$  is the rain rate in  $\text{mm h}^{-1}$ . This  $Z - R$  relationship was derived using vertically pointing MMCR data in drizzling stratocumulus during EPIC [Comstock *et al.*, 2004] and consistent with aircraft in situ measurements in drizzling stratocumulus [Wood, 2005b]. The C-band measurements are compared with the  $r_e$  profile retrieval from MODIS on Terra described below.

## 2.3. Cloud Profile Retrieval Using MODIS

[11] MODIS L1B reflectance measurements at  $\lambda = 0.86$   $\mu\text{m}$ , 1.6  $\mu\text{m}$ , 2.1  $\mu\text{m}$ , and 3.7  $\mu\text{m}$  from Terra satellite are used to estimate cloud optical depth, the  $r_e$  profile, and the LWP using the CL algorithm at a nadir resolution of  $1 \times 1$   $\text{km}^2$ . Only daytime MODIS measurements are used in this study because solar reflectance measurements are needed for retrieving cloud parameters. The Terra overpass time is close to 1600 UTC at 20°S, 85°W, when the solar zenith angle is between 20° and 30° during October. The satellite zenith angle of MODIS ranges between  $-55^\circ$  and  $55^\circ$ .

[12] In the CL algorithm, the linear  $r_e$  profile is defined as a function of height  $z$ , which is defined by

$$r_e(z') = r_{e1} + (r_{e2} - r_{e1})z', \quad (1)$$

where  $z' = (z - z_{\text{top}})/(z_{\text{base}} - z_{\text{top}})$  denotes the fractional cloud height with  $z' = 0$  for the cloud top and  $z' = 1$  for the cloud base. Thus, the linear  $r_e$  profile is parameterized by  $r_{e1}$  at  $z' = 0$  and  $r_{e2}$  at  $z' = 1$  representing the cloud top and cloud base  $r_e$ , respectively. The retrievals of  $r_{e1}$  and  $r_{e2}$  are determined by matching the MODIS measurements with radiative transfer calculations at 3.7, 2.1, and 1.6  $\mu\text{m}$ . Chang and Li [2002] analyzed the potential biases associated with the assumption of a linear  $r_e$  profile and those arising from reflectance error. They showed that the linear  $r_e$  profile retrieval works best for cloud optical depths ranging between 10 and 28. The retrieval mean biases are on the order of 1  $\mu\text{m}$  for cloud top and slightly larger for cloud base if the  $r_e$  profile has a close-to-linear variation. However, if the  $r_e$  variation is very nonlinear, large biases may be incurred, in particular for cloud base  $r_e$ . Also when clouds have large optical depth ( $>28$ ), the quality of  $r_e$  profile estimation does not change much for cloud top but

gets much worse for cloud base because the signal from cloud base is weak for thick clouds. Over all, the uncertainties in  $r_{e2}$  are typically 2–3 times larger than the uncertainties in  $r_{e1}$ .

[13] Traditionally, with the assumption that  $r_e$  is vertically constant, cloud LWP is derived as given by

$$LWP = \frac{4\rho_w}{3Q_e} \tau r_e, \quad (2)$$

Here,  $\tau$  is the cloud optical depth,  $\rho_w$  is the density of liquid water,  $Q_e (=2)$  is the extinction efficiency. Previously,  $r_e$  retrieved with reflectance measurements using a single NIR channel have been used to calculate LWP with equation (2). As discussed earlier, the  $r_e$  retrieved from a single NIR channel like 3.7  $\mu\text{m}$  is more sensitive to the layer near the cloud top, which can cause biases in LWP calculations for cloud with vertical  $r_e$  variation. In the CL algorithm, cloud optical depth is retrieved from MODIS 0.86- $\mu\text{m}$  reflectance measurement for clouds over ocean and LWP is calculated with the linear  $r_e$  profile estimation. Chen *et al.* [2007] showed that MODIS LWP estimation using CL algorithm is consistent with LWP retrieved from AMSR-E microwave observations (i.e., correlation coefficient is around 0.9 for overcast clouds with warm top) and LWP calculation with  $r_e$  profile corrects the biases caused by the assumption of vertically constant  $r_e$ .

## 2.4. Spatial and Temporal Matching of MODIS and C-Band Data

[14] For each RHB location covered by a MODIS scan (a total of five MODIS overpasses during the 6 d during EPIC), the  $r_e$  profile retrievals are compared with coincident RHB scanning C-band radar measurements. MODIS provides instantaneous measurements, while the temporal resolution of the C-band radar is 5 min. To alleviate the influence of the small, but nonnegligible, temporal gap between the two instruments, both MODIS data and C-band data are aggregated and averaged within  $5 \times 5$  km boxes. We aggressively discard aggregated samples that are not fully overcast by insisting that all 25 pixels must contain cloud. There are large uncertainties and ambiguities in retrieval of effective radius if the clouds are very thin (i.e., optical thickness is less than 4) [Nakajima and King, 1990]. In this study, to ensure reliable retrieval of cloud parameters, the optical depths for all cloudy pixels are required to be larger than 4. These constraints have been applied to ensure that as many broken, thin, and highly heterogeneous MODIS pixels (i.e., those most likely to violate the plane-parallel retrieval assumption) are not included in the analysis.

[15] The C-band radar measurements are compared with the  $r_e$  profile retrieval from MODIS on board Terra satellite. As an example of these data, Figure 2 shows coincident images of C-band radar reflectivity, MODIS  $r_e$  profile retrieval (i.e.,  $r_{e1}$  and  $r_{e2}$ ) and MODIS LWP estimates at 1555 UTC of 18 October 2001, a period of strong drizzle also shown in the MMCR data (Figure 1). Data in which cloud is not present or broken, as detailed above, are blanked out. There is considerable heterogeneity in the precipitation field but it is clear that regions of strong drizzle (large  $Z$ ) are generally associated with higher LWP



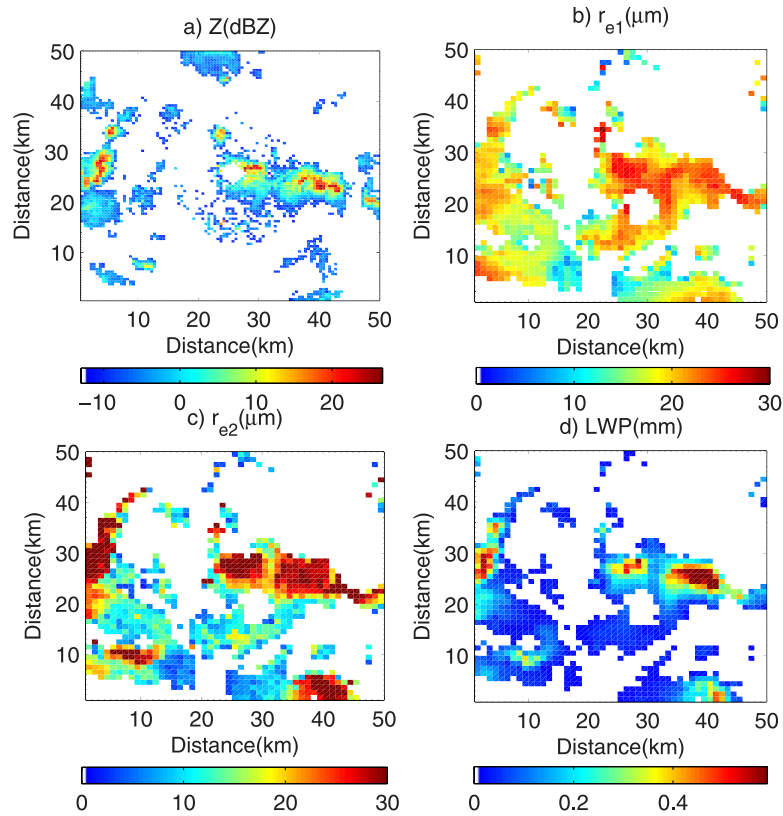


**Figure 2.** Coincident images of C-band radar reflectivity and MODIS cloud profile at UTC 1555, 18 October 2001. (a) RHB C-band radar reflectivity image. (b) MODIS estimation of droplet effective radius at cloud top ( $r_{e1}$ ). (c) MODIS estimation of droplet effective radius at cloud base ( $r_{e2}$ ). (d) MODIS LWP estimation.

and large drops at cloud base (i.e., large  $r_{e2}$ ). There is also a correlation of  $Z$  with the cloud top effective radius  $r_{e1}$  but it is not as clear as with  $r_{e2}$ . This is consistent with the idea that, for heavy drizzle, the drizzle drops themselves may be directly impacting the drop effective radius close to the cloud base. We return to this issue in section 3.2.

### 3. Results

#### 3.1. MMCR Reflectivity Profile and Estimates of the Partitioning of Liquid Water Content Between Drizzle Drops and Small Cloud Droplets

[16] Figure 3 shows the scatterplot of mean radar reflectivity  $Z$  over the upper third ( $0 < z' < 1/3$ ) and lower third ( $2/3 < z' < 1$ ) of the cloud layer, with  $z'$  determined using the cloud top and base heights from the MMCR and ceilometer, respectively. The column maximum reflectivity is shown by the color of the data samples. Radar reflectivity  $Z$  depends the sixth moment of the cloud and drizzle size distribution. Radar reflectivity thresholds for drizzle detection generally range between  $-20$  dBZ and  $-15$  dBZ in previous studies [Sauvageot and Omar, 1987; Wang and Geerts, 2003; Kogan et al., 2005]. For drizzling clouds, the reflectivity due to precipitation drops starts to overwhelm that due to cloud droplets and corresponds to precipitation rates of only a few thousandths of a  $\text{mm hr}^{-1}$ . Thus even modest amounts of precipitation can overwhelm the radar signal due to cloud droplets [Fox and Illingworth, 1997]

even when the drizzle has limited effect on the overall liquid water content and effective radius of the cloud. Figure 3 shows that cloud top  $Z$  is greater than cloud base  $Z$  for nondrizzling clouds (i.e., column maximum reflectivity is

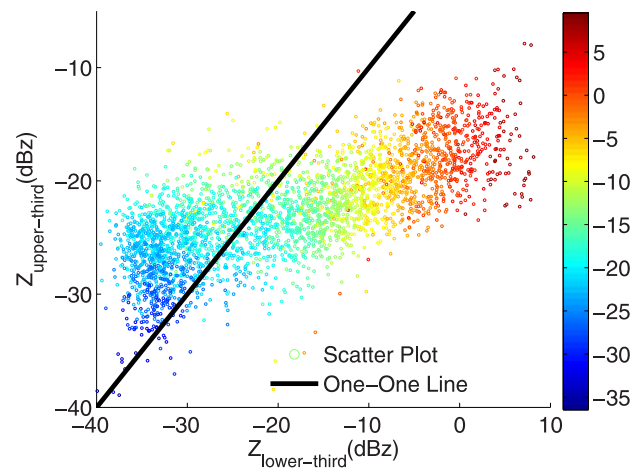


**Figure 3.** Scatterplot of reflectivities over upper 1/3 portion of cloud layer ( $Z_{\text{upper-third}}$ ) and reflectivities over lower 1/3 portion of cloud layer ( $Z_{\text{lower-third}}$ ). Color of the scatterplots represents the column maximum radar reflectivity. The data is from MMCR.

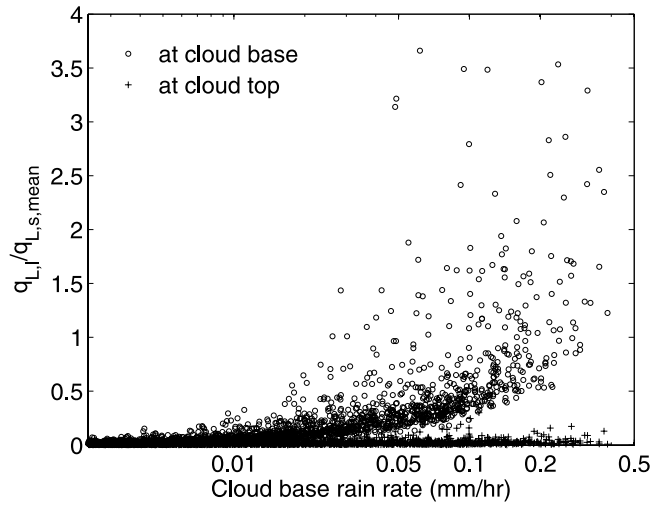


**Figure 4.** Scatterplot of the ratio between the liquid water content of drizzle drops ( $q_{L,l}$ ) and the column mean liquid water content of small droplets ( $q_{L,s,mean}$ ) versus rain rate at cloud base. Circles represent  $q_{L,l,base}/q_{L,s,mean}$  at cloud base and pluses represent  $q_{L,l,top}/q_{L,s,mean}$  at cloud top. The estimates are made with data from shipborne MMCR and microwave radiometer.

–30 dBZ), while the opposite is true for drizzling clouds (i.e., column maximum reflectivity is –10 dBZ) (a result consistent with *Comstock et al.* [2004, Figure 4]). For nondrizzling clouds, cloud droplet size and number concentration determines  $Z$ , and its increase with height is caused primarily by condensational growth of cloud droplets. Drizzle drops dominate radar reflectivity in drizzling clouds. Aircraft observations [*Wood, 2005a*] show that in drizzling stratocumulus the precipitation rate tends to be roughly constant in the lowest two thirds of the cloud layer before decreasing rapidly above this. For drizzling clouds in Figure 3, the large reflectivity in the lower portion of the cloud layer is caused by drizzle at cloud base, while the small radar reflectivity at upper portion of cloud layer is consistent with there being much less drizzle near cloud top.

[17] *Wood* [2000] found that drizzle drops start to increase effective radius significantly if  $\phi = q_{L,l}/q_{L,s}$  is above 0.1, where  $q_{L,l}$  is the liquid water content of large drops ( $r > 20 \mu\text{m}$ ) and  $q_{L,s}$  is the liquid water content of small ( $r < 20 \mu\text{m}$ ) cloud droplets. His study found that it is possible to parameterize the impact of drizzle drops on effective radius as

$$\frac{r_e}{r_{e,s}} \approx \frac{(1 + \phi)^{\frac{2}{3}}}{\left\{ 1 + 0.2 \left( \frac{k_l}{k_s} \right)^{\frac{1}{3}} \phi \right\}} \quad (3)$$

where  $r_e$  is the effective radius for all droplets,  $r_{e,s}$  is the effective radius for small cloud droplets,  $k_l$  is the ratio between the cubes of the volume and effective radius for large drops, and  $k_s$  is the ratio between the cubes of the volume and effective radius for small droplets. In his study,  $k_l$  is parameterized as 2/9 (the exact value for an exponential distribution to which populations of drizzle drops adhere quite closely [*Wood, 2005b*]) and  $k_s$  ranges between

approximately 0.6 and 0.9 [e.g., *Martin et al.*, 1994]. On the basis of equation (3), with the assumption of  $k_s$  equal to 0.75, the drizzle drops would increase  $r_e$  by 40% for  $\phi = 1$  and 10% for  $\phi = 0.2$ . With the MMCR reflectivity profile and the LWP estimation from RHB microwave radiometer, liquid water content of drizzle drops and liquid water content of small cloud droplets can be roughly estimated. The liquid water content of drizzle drops at cloud base is estimated with  $q_{L,l} = \rho R/w_T$ , where  $R$  is cloud base precipitation rate,  $\rho$  is the density of water, and  $w_T$  is the mass-weighted fall speed of drizzle drops. Using a typical fall speed of  $0.4 \text{ m s}^{-1}$  for drizzle drops (consistent with the aircraft data of *Wood* [2005a] for which  $w_T$  is in the range  $0.2\text{--}0.6 \text{ m s}^{-1}$ ), the drizzle liquid water content would be  $q_{L,l} \approx 0.69R$  in  $\text{g m}^{-3}$ . The rain rate profile can be estimated from the MMCR reflectivity profile with  $Z = 25 R^{1.3}$  [*Comstock et al.*, 2004]. Thus, the LWP contributed by drizzle drops ( $LWP_l$ ) is the vertical integral of  $0.69R$  over the depth of the precipitating layer, and LWP contributed by small cloud droplets ( $LWP_s$ ) is estimated by subtracting  $LWP_l$  from total LWP estimated with RHB microwave radiometer measurements. The mean liquid water content of small droplets ( $q_{L,s,mean}$ ) can be estimated from the mean  $LWP_s$  over the cloud depth. Figure 4 shows estimated  $q_{L,l,base}/q_{L,s,mean}$  and  $q_{L,l,top}/q_{L,s,mean}$  against  $R_{cb}$ , where  $q_{L,l,base}$  is the liquid water content of drizzle drops at cloud base,  $q_{L,l,top}$  is the liquid water content of drizzle drops at cloud top, and  $R_{cb}$  is the rain rate at cloud base. It is shown that the  $q_{L,l,base}/q_{L,s,mean}$  grows from  $<0.1$  at  $R_{cb} < 0.01 \text{ mm h}^{-1}$  to  $>1$  as  $R_{cb}$  reaches a few tenths of a  $\text{mm h}^{-1}$ , while  $q_{L,l,top}$  is always much smaller than  $q_{L,s,mean}$ . Because the radius of small cloud droplets generally increases with height,  $q_{L,s}$  at cloud base is expected to be less than  $q_{L,s,mean}$  and  $q_{L,l}/q_{L,s}$  at cloud base is expected to be larger than  $q_{L,l,base}/q_{L,s,mean}$  and so the ratios of drizzle to cloud liquid water presented in Figure 4 are representative of the cloud as a whole and most likely underestimate the impact of drizzle close to cloud base. In any case, taken together with equation (3), such ratios are consistent with drizzle having an impact on the effective radius when the precipitation rate exceeds a few hundredths of a  $\text{mm h}^{-1}$ . It is remarkable that for even relatively modest precipitation rates, a significant fraction of the liquid water content in stratocumulus clouds can reside in drizzle-sized drops. The impacts of drizzle upon  $r_e$  at cloud base could significantly change the trend of vertical  $r_e$  variation because there are not many drizzle drops at cloud top. Using the  $r_e$  profile estimated from satellite reflectance measurements, the following section assesses the impact of drizzle drops on vertical  $r_e$  variation in detail.

### 3.2. Satellite Estimates of the $r_e$ Profile for Drizzling and Nondrizzling Clouds

[18] Figure 5 shows the C-band precipitation rate against the MODIS-derived droplet effective radius at cloud top  $r_{e1}$  and cloud base  $r_{e2}$  for the spatially matched data set from EPIC. A threshold of –12 dBZ (minimum detectable reflectivity of the C-band radar) is used to classify the  $5 \times 5 \text{ km}$  regions into either drizzling or nondrizzling. Statistics of  $r_{e1}$  and  $r_{e2}$  are shown in Table 1. Both  $r_{e1}$  and  $r_{e2}$  are larger for drizzling clouds than for nondrizzling clouds, with a threshold for drizzle of approximately  $15 \mu\text{m}$  in  $r_{e1}$

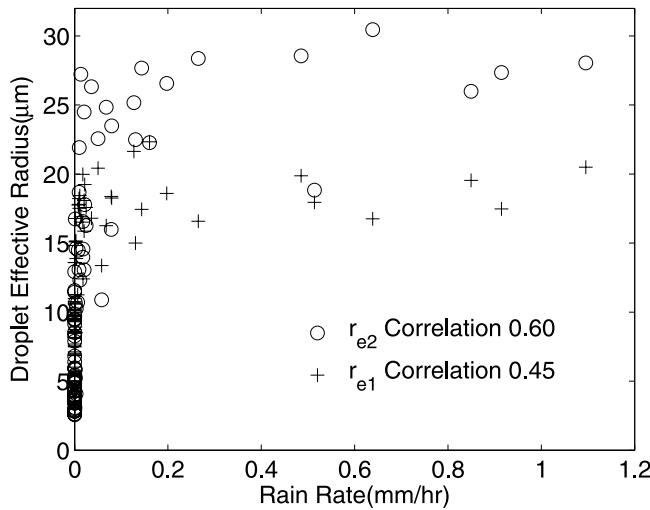


**Figure 5.** Scatterplot between rain rates and cloud droplet effective radius. Here  $r_{e1}$  is droplet effective radius at cloud top and  $r_{e2}$  is droplet effective radius at cloud base. The estimates are made with data from MODIS and C-band radar.

consistent with earlier in situ studies [e.g., Gerber, 1996]. However,  $r_{e2}$  shows a greater contrast between drizzling clouds and nondrizzling clouds. The mean value of  $r_{e1}$  is  $9.6 \mu\text{m}$  for nondrizzling cloud and  $17.1 \mu\text{m}$  for drizzling clouds, while the mean value of  $r_{e2}$  is  $6.3 \mu\text{m}$  for nondrizzling cloud and  $20.8 \mu\text{m}$  for drizzling clouds. The correlation coefficient with rain rate is 0.45 for  $r_{e1}$  and is 0.60 for  $r_{e2}$ . The reason that  $r_{e2}$  is better correlated with rain rate is that the drizzle drops at cloud base increase the effective radius. On the other hand, drizzle decreases markedly toward the cloud top. The correlation between precipitation rate and cloud top effective radius is therefore expected not because the precipitation itself contributes to  $r_e$  but because clouds with large drops near their tops will be more prone to collision-coalescence which ultimately manifests itself as greater precipitation rates lower down in the cloud.

[19] Figure 6 shows the scatterplot between  $r_{e1}/r_{e2}$  and coincident rain rate. Values of  $r_{e1}$  are generally larger than  $r_{e2}$  for nondrizzling clouds and the mean value of  $r_{e1}/r_{e2}$  is 1.61 for nondrizzling clouds. The ratio decreases as the clouds start to drizzle and can become less than unity if drizzle is heavy (i.e., larger than  $0.2 \text{ mm h}^{-1}$ ). The mean rain rate is  $0.04 \text{ mm h}^{-1}$  for drizzling clouds with  $r_{e1}/r_{e2} > 1$  and  $0.18 \text{ mm h}^{-1}$  for drizzling clouds with  $r_{e1}/r_{e2} < 1$ . The mean value of  $r_{e1}/r_{e2}$  is 0.92 for drizzling cloud. The correlation coefficient between  $r_{e1}/r_{e2}$  and rain rate is  $-0.43$ .

[20] Using rain rate estimation from the C-band radar and LWP from MODIS, we can make a rough estimate of  $q_{L,1}/q_{L,s}$  using the same method as in section 3.1. Figure 7

shows a plot of the precipitation rate against LWP. For drizzling cloud, the mean rain rate is  $0.15 \text{ mm h}^{-1}$  and the mean cloud LWP is  $0.16 \text{ mm}$ . As discussed in section 3.1, the drizzle liquid water content would be  $0.69R$  in  $\text{g m}^{-3}$ . The  $0.15 \text{ mm h}^{-1}$  mean rain rate in Figure 7 means a drizzle liquid water content of  $q_{L,1}$  of  $\sim 0.10 \text{ g m}^{-3}$ . The average thickness of a drizzling cloud is around  $0.6 \text{ km}$  for the data used in this study (estimated with MMCR and ceilometer). For an average cloud LWP of  $0.16 \text{ mm}$  in Figure 7, the average cloud liquid water content ( $q_{L,1} + q_{L,s}$ ) is around  $0.25 \text{ g m}^{-3}$  and  $q_{L,s}$  would be around  $0.15 \text{ g m}^{-3}$  after the  $0.10 \text{ g m}^{-3}$   $q_{L,1}$  is subtracted. Considering that  $q_{L,s}$  at cloud base is less than  $q_{L,s}$  at cloud top because  $r_{e1}/r_{e2}$  is larger than 1 without contribution from drizzle drops,  $q_{L,s}$  would be in the same order of magnitude as  $q_{L,1}$  at cloud base for the average rain rate of  $0.15 \text{ mm h}^{-1}$ . Certainly,  $q_{L,1}$  would be smaller than  $q_{L,s}$  when the drizzle is light (i.e.,  $0.01 \text{ mm h}^{-1}$ ) and would be larger than  $q_{L,s}$  when the drizzle is high (i.e.,  $0.5 \text{ mm h}^{-1}$ ).

[21] The above comparison of  $q_{L,1}$  with  $q_{L,s}$  indicates that, for the drizzling clouds in Figure 6, we expect a significant amount of drizzle liquid water content close to cloud base, especially when the precipitation rate exceeds about  $0.1 \text{ mm h}^{-1}$ . Given that the drizzle drops start to increase effective radius significantly if  $q_{L,1}/q_{L,s}$  is above 0.1, the neutralization and conversion of the trends of  $r_e$  vertical variation by drizzle drops in Figure 6 is consistent with theoretical calculations by Wood [2000] and with in situ observations [Martin et al., 1994].

[22] Chen et al. [2007] also suggested similar impact of drizzle on vertical  $r_e$  variation, but in that preliminary study the  $r_e$  decreases with height for most precipitating clouds, and could be either increasing or decreasing for nonprecipitating clouds. As previously stated, this investigation found that most nondrizzling clouds have a  $r_e$  profile that increases with height and drizzling clouds have  $r_e$  profiles that either increase or decrease with height. The differences between the results of the two studies are caused by utilizing different drizzle detection techniques. As stated in section 1, AMSR-E rain detection used in the work of Chen et al. [2007] misses light drizzle and possibly some heavy drizzle if the cloud LWP is low. As a result, the drizzle defined by AMSR-E is necessarily heavy drizzle, while the nondrizzling clouds defined by AMSR-E contain both drizzling and nondrizzling clouds.

#### 4. Summary and Future Studies

[23] Using data from the EPIC 2001 Stratocumulus Study, this study investigates the cloud  $r_e$  vertical variation for drizzling and nondrizzling clouds. Estimates of the partitioning of liquid water content between drizzle drops and small cloud droplets is carried out using MMCR data in drizzling stratocumulus by incorporating simultaneous LWP

**Table 1.** Comparison of Cloud Parameters for Raining Clouds and Nonraining Clouds

	$r_{e1}(\mu\text{m})$	$r_{e2}(\mu\text{m})$	$r_{e1}/r_{e2}$	Cloud LWP (mm)	Rain Rate ( $\text{mm h}^{-1}$ )
Correlation with rain rate	0.45	0.60	-0.44	0.76	N/A
Mean for nonraining clouds	9.6	6.3	1.61	0.034	0
Mean for raining clouds	17.1	20.8	0.92	0.155	0.149



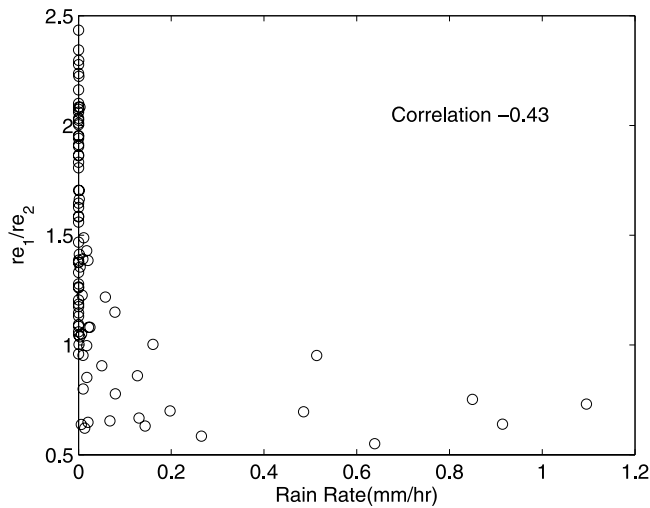


**Figure 6.** Scatterplot between rain rates and ratio between droplet effective radius at cloud top ( $r_{e1}$ ) and droplet effective radius at cloud base ( $r_{e2}$ ). The estimates are made with data from MODIS and C-band radar.

estimates from a passive microwave radiometer. Satellite reflectance measurements from MODIS on the Terra satellite are used to estimate the trend of vertical  $r_e$  variation. Using drizzle rates estimated with a scanning C-band radar we show that the cloud  $r_e$  can decrease with height in clouds with sufficiently strong drizzle. For nondrizzling clouds, the  $r_e$  generally increases with height in accordance with the growth of cloud droplets by condensation. For drizzling clouds, at cloud base, liquid water content of drizzle drops is found to be of comparable magnitude to liquid water content of small cloud droplets when rain rate at cloud base is above a few hundredths of a  $\text{mm h}^{-1}$ . Both previous theoretical analyses [Wood, 2000] and the synergetic observations in this study suggest that drizzle drops can increase  $r_e$  significantly at drizzle rates found in low liquid water clouds. Because drizzle is typically found toward the bottom of these clouds, the  $r_e$  increase by drizzle drops at cloud base can change the trend of vertical  $r_e$  variation and  $r_e$  can decrease with height if drizzle is heavy. On the basis of the radar precipitation observations and satellite cloud  $r_e$  profile estimation,  $r_e$  generally decreases with height when rain rate is above  $0.1 \text{ mm h}^{-1}$ .

[24] Both  $r_e$  at cloud base and  $r_e$  at cloud top are shown to have certain distinction between drizzling and nondrizzling clouds: larger for drizzling clouds than for nondrizzling clouds. The distinction is more striking for  $r_e$  at cloud base than  $r_e$  at cloud top. The  $r_e$  at cloud base is also found to be better correlated with rain rate. The finding of this study suggests that the profile of  $r_e$  or  $r_e$  at cloud base has the potential for drizzle detection in marine low clouds. Drizzle detection is very important in climate studies because drizzle can affect the optical properties of low clouds by changing their macrophysical and microphysical structure [e.g., Albrecht, 1989; Stevens et al., 2005; Wood, 2007]. It is important to develop methodologies for the detection and quantification of drizzle and other light precipitation in low clouds.

[25] Both space-borne passive microwave observations and solar observations have been used for detection of drizzle. Drizzle detection with passive microwave observation uses the estimation of column LWP, which contains both cloud liquid water and drizzle liquid water. The threshold of LWP for drizzle detection is about  $0.2 \text{ mm}$  [Ferraro et al., 1996; Wentz and Spencer, 1998]. Microwave observation has the advantage of being sensitive to drizzle directly, but the ambiguity caused by cloud liquid water may degrade its performance in detection of light drizzle. Zuidema et al. [2005] found that light drizzle is common even at low LWP. Depending upon the microphysical cloud properties such as cloud droplet concentration the column LWP can be very small (i.e.,  $0.05 \text{ mm}$ ) for light drizzle with small rain rate (e.g.,  $0.02 \text{ mm h}^{-1}$  [Wood, 2005a]). On the other hand, the cloud LWP can be as large as  $0.2\text{--}0.4 \text{ mm}$  even for nondrizzling clouds [Wood, 2005a; Berg et al., 2006]. If a  $0.2 \text{ mm}$  threshold of column LWP is applied for drizzle detection, most light drizzle with rain rate less than  $0.1 \text{ mm h}^{-1}$  would be missed. Given that typical precipitation rates in marine low clouds range from  $0.01$  to  $0.1 \text{ mm h}^{-1}$  [e.g., Yum and Hudson, 2002; Wood, 2005a], this detection threshold will miss a significant fraction of drizzling clouds over the oceans. Indeed, results from EPIC show that for these clouds approximately 80% of the drizzling area consists of precipitation rates smaller than  $0.1 \text{ mm h}^{-1}$  and that these weakly drizzling clouds contribute around 25% of the accumulated precipitation at cloud base [Comstock et al., 2004, Figure 9].

[26] Drizzle detection with solar reflectance observations has used cloud  $r_e$  retrieved from single NIR channels. The  $r_e$  threshold for drizzle detection is about  $14 \mu\text{m}$  in previous studies [Rosenfeld and Gutman, 1994; Han et al., 1995]. However, the  $r_e$  retrieved from a single NIR channel is biased toward cloud top, whereas most drizzle is found lower down in the cloud. For example,  $r_e$  retrieval from  $3.7 \mu\text{m}$  represent most top of the cloud layer, while  $r_e$  retrieved from  $2.1 \mu\text{m}$  may represent upper 20% ~40% optical depth of cloud layer with optical depth equal 8 [Nakajima and King, 1990]. As previously stated, between drizzling clouds and nondrizzling clouds, there is a

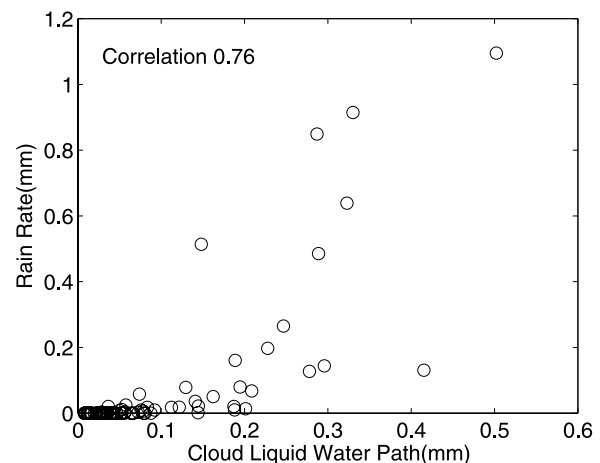


**Figure 7.** Scatterplot between rain rates and liquid water paths. The estimates are made with data from MODIS and C-band radar.

difference in  $r_e$  at cloud top, but a greater contrast in  $r_e$  at cloud base due to the drizzle drops at cloud base for drizzling clouds.

[27] Results of this study shows that satellite  $r_e$  profile estimation ( $r_{e2}$  at cloud base or ratio  $r_{e1}/r_{e2}$ ) could be used as another method for drizzle detection in marine low clouds. The technique details and the quality of the methods beyond the scope of this study because limited data has been available. Future study on this topic could be done when CloudSat data and more campaign data are available.

[28] **Acknowledgments.** EPIC 2001 was a cooperative effort among many scientists, students, staff, and the crew and officers of the R/V *Ronald H Brown*. The authors appreciate their work of acquiring the EPIC 2001 data used in this study. The authors are grateful to the Goddard DAAC for providing MODIS LIB data. This study is supported by the NOAA's GOES-R risk reduction program, the GOES-R algorithm development program, and a grant from the National Basic Research Program of China (2006CB403702). We are grateful to Sandra Yuter (North Carolina State University) and to Kimberly Comstock for their efforts in producing the C-band radar data set.

## References

- Albrecht, B. A. (1989), Aerosols, cloud microphysics and fractional cloudiness, *Science*, *245*, 1227–1230, doi:10.1126/science.245.4923.1227.
- Ashcroft, P., and F. J. Wentz (2000), AMSR algorithm theoretical basis document, *Tech. Rep. 121599B-1*, 27 pp., Remote Sensing Syst., Santa Rosa, Calif.
- Berg, W., T. L'Ecuyer, and C. Kummerow (2006), Rainfall climate regimes: The relationship of regional TRMM rainfall biases to the environment, *J. Appl. Meteorol. Climatol.*, *45*, 434–454, doi:10.1175/JAM2331.1.
- Brenguier, J. L., H. Pawlowska, L. Schüller, R. Preusker, J. Fischer, and Y. Fouquart (2000), Radiative properties of boundary layer clouds: Droplet effective radius versus number concentration, *J. Atmos. Sci.*, *57*, 803–821, doi:10.1175/1520-0469(2000)057<0803:RPOBLC>2.0.CO;2.
- Bretherton, C. S., T. Uttal, C. W. Fairall, S. E. Yuter, R. A. Weller, D. Baumgardner, K. Comstock, and R. Wood (2004), The EPIC 2001 stratocumulus study, *Bull. Am. Meteorol. Soc.*, *85*, 967–977, doi:10.1175/BAMS-85-7-967.
- Chang, F.-L., and Z. Li (2002), Estimating the vertical variation of cloud droplet effective radius using multispectral near-infrared satellite measurements, *J. Geophys. Res.*, *107*(D7), 4257, doi:10.1029/2001JD000766.
- Chang, F.-L., and Z. Li (2003), Retrieving vertical profiles of water-cloud droplet effective radius: Algorithm modification and preliminary application, *J. Geophys. Res.*, *108*(D3), 4763, doi:10.1029/2003JD003906.
- Chen, R., F.-L. Chang, Z. Li, R. Ferraro, and F. Weng (2007), Impact of the vertical variation of cloud droplet size on the estimation of cloud liquid water path and rain detection, *J. Atmos. Sci.*, *64*, 3843–3853.
- Comstock, K. K., R. Wood, S. E. Yuter, and C. S. Bretherton (2004), Reflectivity and rain rate in and below drizzling stratocumulus, *Q.J.R. Meteorol. Soc.*, *130*, 2891–2918, doi:10.1256/qj.03.187.
- Ferraro, R. R., N. C. Grody, F. Weng, and A. Basist (1996), An eight-year (1987–1994) time series of rainfall, clouds, water vapor, snow cover, and sea ice derived from SSM/I measurements, *Bull. Am. Meteorol. Soc.*, *77*, 891–906, doi:10.1175/1520-0477(1996)077<0891:AEYTSO>2.0.CO;2.
- Fox, N. I., and A. J. Illingworth (1997), The retrieval of stratocumulus cloud properties by ground-based cloud radar, *J. Appl. Meteorol.*, *36*, 485–492, doi:10.1175/1520-0450(1997)036<0485:TROSCP>2.0.CO;2.
- Gerber, H. (1996), Microphysics of marine stratocumulus clouds with two drizzle modes, *J. Atmos. Sci.*, *53*(12), 1649–1662, doi:10.1175/1520-0469(1996)053<1649:MOMSCW>2.0.CO;2.
- Greenwald, T. J., G. L. Stephens, S. A. Christopher, H. Vonder, and H. Thomas (1995), Observations of the global characteristics and regional radiative effects of marine cloud liquid water, *J. Clim.*, *8*, 2928–2946, doi:10.1175/1520-0442(1995)008<2928:OOTGCA>2.0.CO;2.
- Han, Q., W. B. Rossow, and A. A. Lacis (1994), Near-global survey of effective droplet radii in liquid water clouds using ISCCP data, *J. Clim.*, *7*, 465–497, doi:10.1175/1520-0442(1994)007<0465:NGSOED>2.0.CO;2.
- Han, Q., W. B. Rossow, R. Welch, A. White, and J. Chou (1995), Validation of satellite retrievals of cloud microphysics and liquid water path using observation from FIRE, *J. Atmos. Sci.*, *52*, 4183–4195, doi:10.1175/1520-0469(1995)052<4183:VOSROC>2.0.CO;2.
- King, M. D., W. P. Menzel, Y. J. Kaufman, D. Tanre, B. C. Gao, S. Platnick, S. A. Ackerman, L. A. Remer, R. Pincus, and P. A. Hubanks (2003), Cloud and aerosol properties, precipitable water, and profiles of temperature and humidity from MODIS, *IEEE Trans. Geosci. Remote Sens.*, *41*, 442–458, doi:10.1109/TGRS.2002.808226.
- Klein, S. A., and D. L. Hartmann (1993), The seasonal cycle of low stratiform clouds, *J. Clim.*, *6*, 1587–1606, doi:10.1175/1520-0442(1993)006<1587:TSCOLS>2.0.CO;2.
- Kobayashi, T. (2007), Significant differences in the cloud droplet effective radius between nonprecipitating and precipitating clouds, *Geophys. Res. Lett.*, *34*, L15811, doi:10.1029/2007GL029606.
- Kogan, Z. N., D. B. Mechem, and Y. L. Kogan (2005), Assessment of variability in continental low stratiform clouds based on observations of radar reflectivity, *J. Geophys. Res.*, *110*, D18205, doi:10.1029/2005JD006158.
- Martin, G. M., D. W. Johnson, and A. Spice (1994), The measurement and parameterization of effective radius of droplets in warm stratocumulus clouds, *J. Atmos. Sci.*, *51*, 1823–1842, doi:10.1175/1520-0469(1994)051<1823:TMAPOE>2.0.CO;2.
- Miles, N. L., J. Verlinde, and E. E. Clothiaux (2000), Cloud droplet size distributions in lowlevel stratiform clouds, *J. Atmos. Sci.*, *57*, 295–311, doi:10.1175/1520-0469(2000)057<0295:CDSDIL>2.0.CO;2.
- Moran, K. P., B. E. Martner, M. J. Post, R. A. Kropfli, D. C. Welsh, and K. B. Widener (1998), An unattended cloud-profiling radar for use in climate research, *Bull. Am. Meteorol. Soc.*, *79*, 443–455, doi:10.1175/1520-0477(1998)079<0443:AUCPRF>2.0.CO;2.
- Nakajima, T., and M. D. King (1990), Determination of the optical thickness and effective particle radius of clouds from the reflected solar radiation measurements. Part I: Theory, *J. Atmos. Sci.*, *47*(15), 1878–1893, doi:10.1175/1520-0469(1990)047<1878:DOTOTA>2.0.CO;2.
- Platnick, S. (2000), Vertical photon transport in cloud remote sensing problems, *J. Geophys. Res.*, *105*, 22,919–22,935, doi:10.1029/2000JD900333.
- Rosenfeld, D., and G. Gutman (1994), Retrieving microphysical properties near the tops of potential rain clouds by multispectral analysis of AVHRR data, *Atmos. Res.*, *34*, 259–283, doi:10.1016/0169-8095(94)90096-5.
- Sauvageot, H., and J. Omar (1987), Radar reflectivity of cumulus clouds, *J. Atmos. Oceanic Technol.*, *4*, 264–272, doi:10.1175/1520-0426(1987)004<0264:RROCC>2.0.CO;2.
- Stevens, B., G. Vali, K. Comstock, R. Wood, M. C. van Zanten, P. H. Austin, C. S. Bretherton, and D. H. Lenschow (2005), Pockets of open cells and drizzle in marine stratocumulus, *Bull. Am. Meteorol. Soc.*, *86*, 51–57, doi:10.1175/BAMS-86-1-51.
- VanZanten, M. C., B. Stevens, G. Vali, and D. H. Lenschow (2005), Observations of drizzle in nocturnal marine stratocumulus, *J. Atmos. Sci.*, *62*, 88–106, doi:10.1175/JAS-3355.1.
- Wang, J., and B. Geerts (2003), Identifying drizzle within marine stratus with W-band radar reflectivity, *Atmos. Res.*, *69*, 1–27, doi:10.1016/j.atmosres.2003.08.001.
- Wentz, F. J., and R. W. Spencer (1998), SSM/I rain retrievals within a unified all-weather ocean algorithm, *J. Atmos. Sci.*, *55*, 1613–1627, doi:10.1175/1520-0469(1998)055<1613:SSIRWA>2.0.CO;2.
- Wood, R. (2000), Parameterization of the effect of drizzle upon the droplets effective radius in stratocumulus clouds, *Q.J.R. Meteorol. Soc.*, *126*, 3309–3324, doi:10.1002/qj.49712657015.
- Wood, R. (2005a), Drizzle in stratiform boundary layer clouds. Part I: Vertical and horizontal structure, *J. Atmos. Sci.*, *62*, 3011–3033, doi:10.1175/JAS3529.1.
- Wood, R. (2005b), Drizzle in stratiform boundary layer clouds. Part II: Microphysical aspects, *J. Atmos. Sci.*, *62*, 3034–3050, doi:10.1175/JAS3530.1.
- Wood, R. (2007), Cancellation of aerosol indirect effects in marine stratocumulus through cloud thinning, *J. Atmos. Sci.*, *64*, 2657–2669, doi:10.1175/JAS3942.1.
- Yum, S. S., and J. G. Hudson (2002), Maritime/continental microphysical contrasts in stratus, *Tellus, Ser. B*, *54*, 61–73.
- Zuidema, P., E. R. Westwater, C. Fairall, and D. Hazen (2005), Ship-based liquid water path estimates in marine stratocumulus, *J. Geophys. Res.*, *110*, fD20206, doi:10.1029/2005JD005833.

F.-L. Chang, National Institute for Aerospace, Hampton, VA 23666, USA.

R. Chen and Z. Li, Department of Atmospheric and Oceanic Sciences, University of Maryland, College Park, MD 20742, USA. (zli@atmos.umd.edu)

R. Ferraro, Cooperative Institute for Climate Studies, University of Maryland, College Park, MD 20742, USA.

R. Wood, Department of Atmospheric Sciences, University of Washington, Seattle, WA 98195, USA.